

THE HIGH-ENERGY PICTURE OF GRS 1915+105 WITH SPI/INTEGRAL

Droulans, R.¹ and Jourdain, E.¹

Abstract. We report the results of two years of INTEGRAL/SPI monitoring of the Galactic microquasar GRS 1915+105. From July 2004 to May 2006, the source has been observed twenty times with long (~ 100 ks) exposures. We present an analysis of the SPI data and focus on the description of the high-energy (> 20 keV) output of the source. We find the 20–500 keV spectral emission of GRS 1915+105 to be bounded between two limit states. In particular, it seems that these high-energy states are not correlated to the temporal behavior of the source, suggesting that there is no immediate link between the macroscopic characteristics of the coronal plasma and the variability of the accretion flows. All spectra are well fitted by a thermal comptonization component plus an extra high-energy powerlaw. This confirms the presence of thermal and non-thermal electrons around the black hole.

1 Introduction

GRS 1915+105 is among the most notorious accreting black holes in our Galaxy. Not only it is one of the brightest and most variable X-ray sources in the sky (see Castro-Tirado et al. 1992 for a first detection report and Belloni et al. 2000 for detailed variability analysis), but it is also the first galactic object in which superluminal plasma ejections have been observed (Mirabel & Rodriguez 1994).

Yet, most of the recent studies (see Fender & Belloni 2004 for a review) focus on the astonishing X-ray properties, the soft γ -ray emission (> 100 keV) being generally observed at poor signal to noise ratio. Understanding the high-energy behavior of the source is nevertheless very important as it is assumed to trace the physical processes occurring at the innermost regions surrounding the black-hole (e.g. Galeev et al. 1979 or Malzac 2007 for a review). Featuring good spectral resolution and sensitivity up to several *MeV*, the γ -ray spectrometer SPI (Vedrenne et al. 2003) aboard the INTEGRAL observatory is a good instrument to tackle this issue.

Here we present all SPI observations on GRS 1915+105 from July 2004 to May 2006. We focus on gaining the most accurate high-energy picture of the source, mainly through extensive spectral analysis. Emphasis is given to four observations which we found to be of particular interest.

2 Results

From July 2004 to May 2006, the source has been observed twenty times with long (~ 100 ks) exposures. The total 20–50 keV light-curve from our observational period shows relevant long-term variability, the averaged source flux per observation (\approx one-day) spanning between 90 and 380 *mCrab*. On the shorter science-window timescale (≈ 2 ks), the obtained individual light-curves show generally lower variability. Within a single observation, the source flux varies at most by a factor of 2. As GRS 1915+105 is well known for being very variable in X-rays, we also considered SPI-simultaneous 1.2–12 keV ASM light-curves to compare the X- and soft γ -ray behavior of the source. We used XSPEC 11.3.2 (Arnaud 1996) for spectral analysis. Each observation-averaged spectrum is fitted with a basic powerlaw model which gives a good description of most of the data. The photon index is found to range from 2.8 to 3.5.

2.1 Observations 295 and 423

From the ASM light-curves (figure 1 left), we see that for both observations GRS 1915+105 shows very similar X-ray activity, summarily characterized by low flux and almost no variability. The temporal properties in the 20–50 keV band

¹ CESR / CNRS – Université de Toulouse, 9 Av. du Colonel Roche, 31028 Toulouse Cedex 04, France

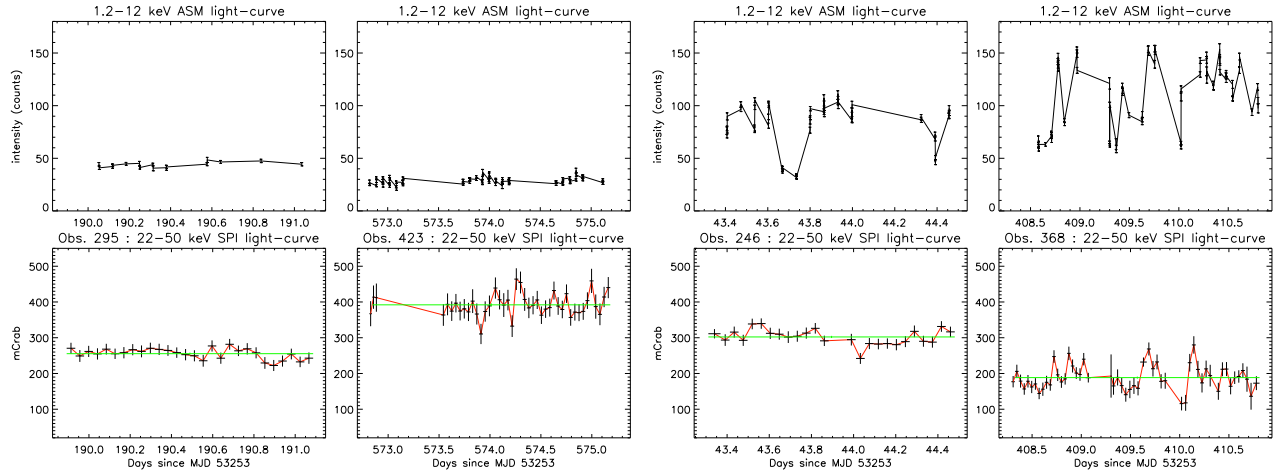


Fig. 1. ASM and SPI light-curves. **Left** : Observations 295 and 423. **Right**: Observations 246 and 368.

are also quite alike, with little variability during both observations. However, spectral characteristics are found to be significantly different, with respective photon indices of 3.5 and 2.8. We will now further investigate these differences through more detailed spectral modelling.

A simple powerlaw model gives a rather poor fit for observation 295. Pure thermal comptonization models like COMPTT (Titarchuk 1994) can also be ruled out ($\chi^2/\nu = 72/26$). Assuming that the low-energy part is nonetheless produced through thermal comptonization, one needs to add a further spectral component. We thus chose to add a powerlaw as a phenomenological description of the observed high-energy tail. Given the error amplitude above 100 keV, we arbitrarily fixed the photon index to the standard value 2.0. The resulting fit ($kT_e = 16.3$ keV and $\tau = 0.57$) is in very good agreement with our data ($\chi^2/\nu = 17/25$) and the *F-TEST* indicates a probability of $\sim 10^{-9}$ that this improvement has been a chance event. As a last step we applied Poutanen and Svensson's COMPPS model (1996). Note that COMPPS is more constraining than COMPTT+PL as it requires both components (thermal and non-thermal) to be linked, whereas the former does not. Equally good fitting results ($\chi^2/\nu = 17/25$) for both models confirmed the observed 20–500 keV emission to most likely originate from thermal and non-thermal comptonization processes.

For observation 423, the basic powerlaw fit is clearly unacceptable ($\chi^2/\nu = 83/27$) due to the marked curvature around 50 keV, leaving clear evidence for thermal processes. However, a thermal component alone is not able to account for the observed emission above 200 keV. We thus keep the hybrid comptonization models ($\chi^2/\nu = 37/25$ for COMPTT+PL and $\chi^2/\nu = 37/24$ for COMPPS) as our preferred description for the spectrum from observation 423.

2.2 Observations 246 and 368

Considering the (2 ks timescale) lightcurves from observation 368, we find the same variability pattern in X-rays as in the 20–50 keV SPI band (figure 1 right), indicating that both bands are probably sampling the temporal behavior of the same component. For observation 246 there seems to be a similar correspondence, although less clear due to lower variability amplitude in the SPI band. Both spectra are fitted with thermal + non-thermal comptonization models (COMPTT+PL and COMPPS) which provide the best agreement to the data.

2.3 Composite spectra

In order to go further in the description of the high-energy tail of GRS 1915+105, we decided to compile consistent information from different observations. Improved statistics on the resulting composite spectra would indeed allow us to put better constraints on the parameters of the fitted models. The first group of observational data is characterized by a rather low 20–50 keV flux (~ 200 mCrab) and a very soft spectral shape ($\Gamma \approx 3.45$); hereafter we will call it the *soft sample*. The second group on the other hand has hard colors ($\Gamma \approx 2.90$) and a high flux (~ 330 mCrab) in the 20–50 keV band; it will accordingly be called the *hard sample*. As a result, our two samples are likely to describe the boundary comptonization states between which the source seems to be continuously switching.

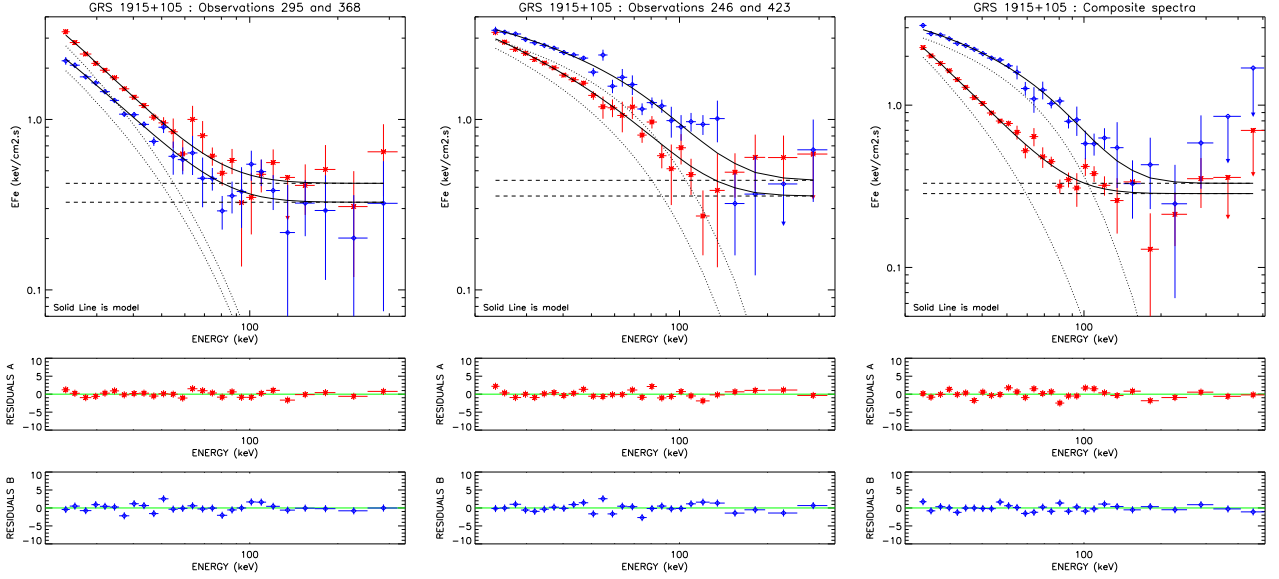


Fig. 2. COMPTT+PL best fits. **Left** : Observations 295 (red stars) and 368 (blue diamonds). **Middle** : Observations 246 (red stars) and 423. **Right** : Soft sample (red stars) and hard sample.

Obs ID	COMPTT						PL				
	kT_{bb} (keV)	kT_e (keV)	τ	γ_{\min}	Γ_e	F_{comptt}	α	K_{pl}	χ^2/ν	FTEST	
246	1.0f	$18.2^{+1.1}_{-1.0}$	0.97	-	-	3.64	2.0f	$3.48^{+1.05}_{-0.96}$	27/25	4×10^{-2}	
295	1.5f	$16.3^{+1.2}_{-0.9}$	0.57	-	-	2.73	2.0f	$3.95^{+0.66}_{-0.56}$	17/25	2×10^{-9}	
368	1.5f	$13.4^{+1.0}_{-0.9}$	0.86	-	-	1.94	2.0f	$3.28^{+0.54}_{-0.56}$	29/25	1×10^{-6}	
423	1.0f	$19.2^{+1.0}_{-1.0}$	1.20	-	-	4.91	2.0f	$4.27^{+1.29}_{-1.38}$	37/25	8×10^{-2}	
SS	1.5f	$16.5^{+0.6}_{-0.6}$	0.62	-	-	2.07	2.0f	$2.75^{+0.28}_{-0.29}$	31/25	3×10^{-10}	
HS	1.0f	$17.7^{+0.7}_{-0.7}$	1.28	-	-	4.13	2.0f	$3.31^{+0.91}_{-0.95}$	19/25	8×10^{-4}	

Table 1. Spectral fitting of the four highlighted observations and the composite samples. For each spectrum the COMPTT + PL parameters are given. Seed photon temperature is fixed to standard values. COMPTT errors are calculated on kT_e while fixing τ to its best fit value. F_{comptt} denotes the integrated 20-500 keV energy flux from the thermal component and is given in units of $\times 10^{-9} \text{ ergs/cm}^2/\text{s}$. K_{pl} is the flux normalization at 100 keV of the non-thermal powerlaw and is given in units of $\times 10^{-5} \text{ photons/cm}^2/\text{s/keV}$

3 Discussion

We interpret the 20–500 keV emission of GRS 1915+105 as a conjunction of thermal and non-thermal comptonization. Given the similarities of the observed temporal properties, the ASM band is likely to sample the same emission component as the 20–50 keV SPI band. This is in agreement with the results of Done et al. (2004) who show that except for ultrashort disc-dominated X-ray spikes the accretion disc has no significant effect above 3 keV (see also Rodriguez et al. 2008). The spectra obtained during observations 295 and 368 on one hand and 246 and 423 on the other show that for different X-ray classes (i.e. different temporal behavior of the hot accretion flow) the high energy spectra can be very similar. Conversely, observations 295 and 423 show that within stable emission episodes, there can be significant differences in the spectral behavior of the source. Assuming that the 3–50 keV emission originates from the comptonizing corona (see Malzac 2007 or Done et al. 2007 for details), this clearly indicates that there is no correlation between the temporal variability and the macroscopic properties of the comptonizing accretion flow.

3.1 The limit states

Modelling the soft sample spectrum reveals the intersection point of the two components to be around 60 keV . At higher energies, the non-thermal processes dominate. Both the thermal and non-thermal components have approximately the same luminosity above 20 keV . If these two components originate from the same population, the electrons are found to thermalize around Lorentz factor $\gamma_{min} = 1.3$. The mildly hot Compton cloud ($kT_e \approx 15\text{ keV}$) is found to be marginally optically thick ($\tau \approx 2.7$) which is an expected configuration for black-hole binaries in a very high state (Done & Kubota 2006). We suggest that our soft composite spectrum gives a template high-energy representation of GRS 1915+105 in low coronal luminosity states.

Concerning the hard sample spectrum, the luminosity of the non-thermal component is found to be roughly the same as for the previously discussed soft sample. However, the intersection point of the two components is now around 110 keV (which corresponds to Lorentz factor $\gamma_{min} \approx 1.39$), showing that the main difference lies in the properties of the comptonizing thermal electrons of the corona. The plasma is found to be either hotter for similar optical depth or optically thicker for similar electron temperature (or a mixture of both), thus enhancing the higher observed $20\text{--}50\text{ keV}$ flux. Even though this situation cannot be completely resolved due to the observational $kT\text{--}\tau$ degeneracy, spectral fits with COMPPS indicate that most probably there has been a significant increase in opacity, whereas electron temperature remains between 14 and 18 keV . In any case, this does not affect the estimation of the total $20\text{--}500\text{ keV}$ luminosity issued from thermal Compton scatterings, which is found to be enhanced at least by a factor of 2 in comparison with the soft sample. We interpret our spectrum as a template for the high-energy emission of GRS 1915+105 in high coronal luminosity states.

4 Summary and Conclusion

We have conducted detailed high-energy spectral analysis of the GRS 1915+105 microquasar through all available SPI data from July 2004 to May 2006. We can summarize our findings as follows:

We found the \sim one day averaged $20\text{--}500\text{ keV}$ spectral emission to be always between two boundary states, *hard* and *soft*, which we illustrated through spectral modelling. We confirm that INTEGRAL-SPI observes no high-energy cutoff for GRS 1915+105 (Rodríguez et al. 2008). More precisely, we suggest that the high-energy cutoff from thermal comptonization is drowned by an additional non-thermal component. We found the non-thermal component to be statistically required in both composite samples. The spectral differences we observed in hard X-rays ($20\text{--}50\text{ keV}$) are most likely coupled to the evolution of the thermal electron plasma. The bolometric luminosity issued out of thermal comptonization varies by a factor of 2 between soft and hard samples. In contrast, the obtained fits indicate that the non-thermal component is rather stable. This implies that both components are not necessarily linked, i.e. they could originate from dissociated electron populations. Given the length of the high-energy observations (SPI $\approx 3\text{ days}$ or OSSE $\approx 15\text{ days}$), it is difficult to investigate the connections between the various X-ray classes and the high-energy spectra. Yet we pointed out that there is no direct correlation between the observed variability patterns and our $20\text{--}500\text{ keV}$ SPI spectra. This shows that the macroscopic properties of the comptonizing thermal electrons evolve independently from the temporal behavior of the source, i.e. independently from the fluctuations of the accretion flow.

References

- Arnaud, K.A., 1996, in Jacoby, G.H., Barnes, J., eds, ASP Conf. Ser. Vol.101, San Francisco, p.17
- Belloni, T., Klein-Wolt, M., Méndez M., et al. 2000, A&A, 355, 271
- Castro-Tirado, A.J., Brandt S., & Lund, N. 1992, IAUC, 5590, 2
- Done, C., Wardziński, G., & Gierliński, M. 2004, MNRAS, 349, 393
- Done, C. & Kubota, A. 2006, MNRAS, 371, 1216
- Done, C., Gierliński, M., & Kubota, A., 2007, A&AR Volume 15, Issue 1, 1
- Fender, R.P., & Belloni, T. 2004, ARA&A, 42, 317
- Galeev, A.A., Rosner, R., & Vaiana, G.S. 1979, ApJ, 229, 318G
- Malzac, J. 2007, ApJS, 170, 175
- Mirabel, I.F., & Rodríguez, L.F. 1994, Nature, 371, 46
- Poutanen, J., & Svensson, R. 1996, ApJ, 470, 249
- Rodríguez, J., Shaw, S.E., Hannikainen, D.C. et al. 2008, ApJ, 675, 1449R
- Titarchuk, L. 1994, ApJ, 434, 313
- Vedrenne, G., Roques, J.P, Schönfelder, et al. 2003, A&A, 411, L63